Investigations of Strength and Energy Absorption of Clinched Joints

Xiaocong He[1)], Lun Zhao[1)], Huiyan Yang[1)], Baoying Xing[1)], Yuqi Wang[1)],

Chengjiang Deng[1)], Fengshou Gu[2)], Andrew Ball[2)]

1) Innovative Manufacturing Research Centre, Kunming University of Science and Technology, Kunming, 650093, P. R. China
2) Centre for Efficiency and Performance Engineering, University of Huddersfield, Queensgate, Huddersfield, HD1 3DH, UK.

Abstract

With an increasing application of clinching in different industrial fields, the demand for a better understanding of the knowledge of static and dynamic characteristics of the clinched joints is required. In this paper, the clinching process and tensile-shear failure of the clinched joints have been numerically simulated using finite element (FE) method. For validating the numerical simulations, experimental tests on specimens made of aluminium alloy have been carried out. The results obtained from tests agreed fairly well with the computational simulation. Tensile-shear tests were carried out to measure the ultimate tensile-shear strengths of the clinching joints and clinching-bonded hybrid joints. Deformation and failure of joints under tensile-shear loading were studied. The normal hypothesis tests were performed to examine the rationality of the test data. This work was also aimed at evaluating experimentally and comparing the strength and energy absorption of the clinched joints and clinching-bonded hybrid joints.

Keywords: Clinching; Numerical simulation; Finite element method; Tensile-shear failure; Load-bearing capacity; Energy absorption.

Corresponding author: Tel. : +86-871-65930928

E-mail address: hhxxcc@yahoo.co.uk

1. Introduction

Advanced joining technology is an integral part of the manufacturing processes of lightweight structures. Many efforts have been spent to develop the suitability of various joining processes for application into lightweight structures [1-4]. Clinching has also been developed rapidly into a new branch of mechanical joining techniques [5. 6]. Clinching is a high-speed mechanical fastening technique which is suitable for point joining advanced lightweight sheet materials that are dissimilar, coated and hard to weld. The use of clinching is of great interest to many industrial sectors including aerospace and automotive. This, together with increasing use of light weight materials which normally are difficult or impossible to weld, has produced a significant increase in the use of clinching technology in engineering structures and components in recent years.

The static and dynamic behaviour of clinched joints has been the subject of a considerable amount of experimental and numerical studies. A study on the joining mechanism of clinching has been conducted by Gao and Budde [7]. Some basic terms, such as the mechanical contact chains and their symbols and the joint networks, were introduced to establish a basic theory for analysing the joining mechanism. In Zheng et al.'s paper [8], the extensible die clinching process has been simulated using finite element (FE) method. The material flowing patterns have been compared between the fixed grooved die clinching and the extensible die clinching. The process monitoring systems are able to distinguish between accidental and systematic process errors and can, therefore, keep unnecessary plant stops to a minimum and ensure high levels of plant availability [9]. The influence of process parameters in extensible die clinching has been systematically investigated by Lambiase and colleague [10, 11]. Clinched joints were produced under different forming loads to evaluate the evolution of the joints' profile experimentally. The suitability and economics of clinching processes have been studied by Varis [12, 13]. In another work, Varis pointed out several problems encountered in the long-term use of a clinching process and both the lack of systematic maintenance, and continuous follow-up were discussed [14]. Mori et al [15] carried out a comparison between the static and fatigue behaviour of joints produced with clinching and self-piercing riveting.

The clinching process is a method of joining sheet metal or extrusions by localized cold forming of materials. The result is an interlocking friction joint between two or more layers of material formed by a punch into a special die. It is believed that the clinched joints act to augment the system damping capacity. In spite of the fact that the clinched joints have been widely used in manufacturing practice, the reports about energy absorption of the clinched joints have never been seen in

previous literature. Recent work by present author and coworkers investigated the energy effect in the vibration analysis of the clinched joints [16]. Due to the complex clinched joint geometry and its three dimensional nature, it is difficult to obtain governing equations for predicting the mechanical properties of clinch joints. The experimental predictions are time-consuming and expensive. To overcome these problems, the FE method is increasingly used in recent decades. In this paper, the clinching process and clinched joint tensile-shearing have been numerically simulated using the commercial FE analysis software. Axisymmetric FE models were generated based on the Cowper-Symonds material models. An implicit solution technique with Lagrange method and *r*-self-adaptivity was used. For validating the numerical simulations of the clinching process and clinched joint tensile-shearing, experimental tests on specimens made of aluminium alloy 7075 were carried out. The structural analysis has also been performed for comparing load-bearing capacity and energy absorption of clinched joints and clinching-bonded hybrid joints.

2. Computational and Experimental Studies of Clinching Process

2.1 Numerical simulation of clinching process

A 2D axisymmetric model was generated using the commercial FE software LS-Dyna. The von Mises yield criterion, the piecewise linear isotropic strain-hardening rule, and the associated flow rule were adopted in the plastic domain. Since clinching process involves large deformation, elements may become severely distorted. Distorted meshes are less accurate and may accordingly introduce numerical difficulties. For avoiding numerical problems due to mesh disturbances, the efficacious approach is to use an erosion or element kill technique. The element kill technique corresponds to the progressive removal of the fully damaged elements. When the elements are removed, the interfaces between the sheets and other parts become rough. For getting smoother interfaces, a small element size is required. However, a small element size increases the number of elements in the simulation and the time of the simulation. To take the whole situation into account, an implicit solution technique with Lagrange method and *r*-self-adaptivity has been used.

As shown in Fig. 1, a single lap clinched joint comprises an upper sheet, lower sheet. The sheet materials tested were 7075 aluminium alloy sheets of dimensions 110 mm length ×20 mm width ×2 mm thickness and were clinched together in the central part of lap section. The mechanical properties of the aluminium alloy sheets were as follow: Young's modulus, E=68 GPa; Poisson's ratio, v=0.33.

Fig. 2 shows the FE model of clinching process. The punch, blank holder and die were modelled as rigid bodies, while the sheets were modelled as elasto-plastic materials. The piecewise-linear plasticity material model which adopts the Cowper-

Symbols model to consider the influence of strain rate was used. The relationship between the Cowper-Symbols model and yield stress is shown in the following equation:

$$\sigma_y = [1 + \left(\frac{\dot{\varepsilon}^t}{C}\right)^{\frac{1}{P}}](\sigma_0 + f(\varepsilon_{eff}^P)) \quad (1)$$

Where σ_0 is the yield stress in constant strain rate, $\dot{\varepsilon}^t$ is the effective strain rate, C and P are the parameters of strain rate; $f(\varepsilon_{eff}^P)$ is the hardening coefficient which is based on the effective plastic strain.

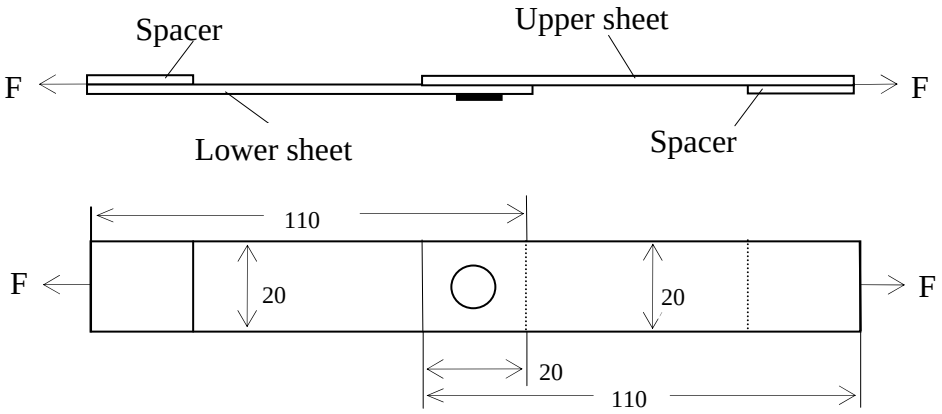

Fig. 1. Configuration and boundary condition of a single lap clinched joint (dimensions in mm)

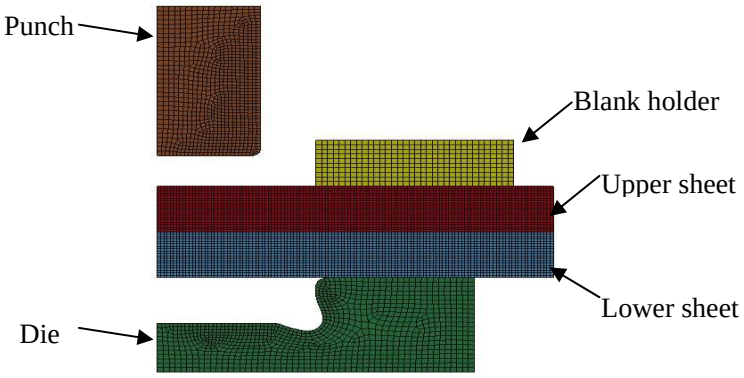

Fig. 2. FE model of clinching

The friction between different parts in the model has an influence on the results of the simulation and the best value of the friction is not consistent for all the simulations. In the lack of experimental data, tentative values of the Coulomb friction coefficient between different parts in the model were assumed as follows: f=0.25 punch-upper sheet, f=0.15 upper sheet-blank holder, f=0.15 upper sheet-lower sheet, f=0.25 lower sheet-die. These values were kept constant for all simulations in this study.

The clinching process was simulated by applying a specified downward initial velocity to every node within the punch. Fig. 3 shows the FE simulation of clinching process and Fig. 4 shows the pressure-time curve of typical element in the simulation.

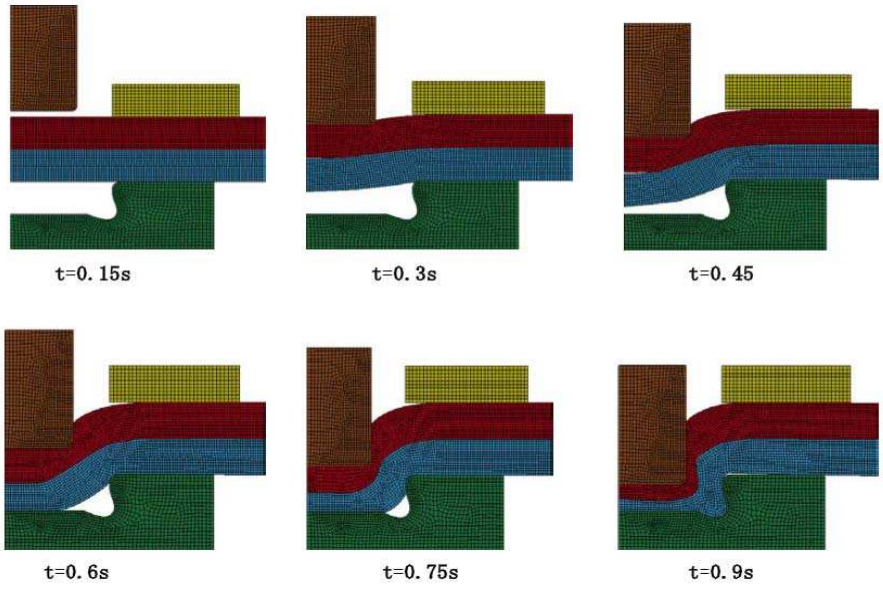

Fig. 3 FE simulation of clinching process

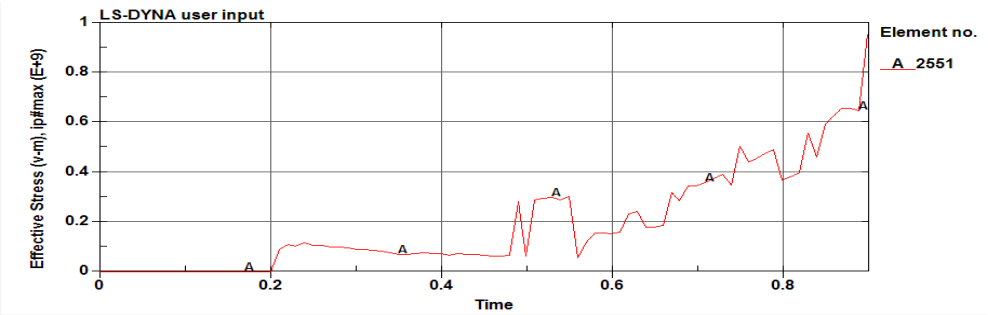

Fig.4. Pressure-time curve of a typical element in clinching process

2.2 Clinching process tests

A clinching equipment RIVCLINCH 1106 P50 system was employed as clinching machine. All clinched joints were made with constant pre-clamp (5 kN) and

setting (50 kN) load. A clinched joint was cut from the centreline of the clinch point perpendicular to the length of the specimen. Fig. 5 shows the cross-section comparison between simulations and tests of clinching processes. A reasonable agreement between the simulations and the tests was found. However a little difference between the simulation prediction and experimental measurement can be observed regarding the thicknesses of sheets at the bottom of clinched point. Such a discrepancy can be attributed to the neglecting of the material transverse anisotropy in the simulation prediction. The results show the capability of the 2D LS-Dyna axisymmetric model to simulate the clinching process for different geometries and work conditions.

As is well known, it is difficult to display the grains of aluminium alloy by normal chemistry etching. The electrolytic polishing and anode film coating were used for dealing with the cross-section, then the differential interference contrast (DIC) method was used for observing the microstructure of the cross-section of the clinched joints. Fig. 6 shows a variation in grain size and shape from un-deformed zone, to mechanically affected zone, then to sheet-sheet contacted zone and sheet-die contacted zone. The average grain size ranges from around 48 μm at un-deformed zone to around 26 μm at mechanically affected zone then to around 12 μm at sheet-sheet contacted zone and sheet-die contacted zone. The grain shape changes from equiaxed grain to streaky grain.

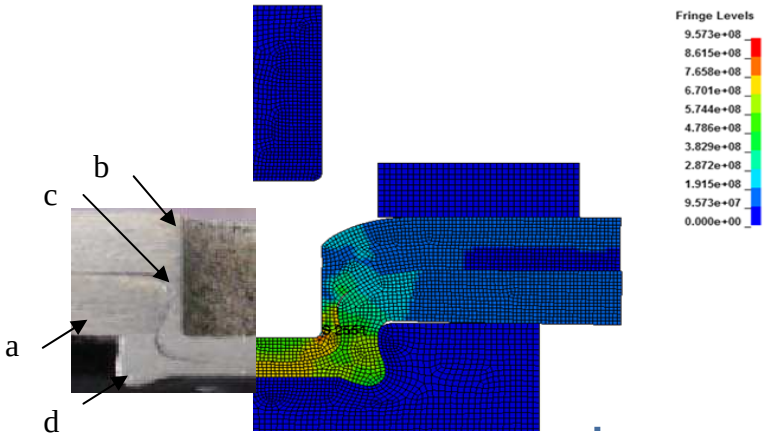

Fig.5. Cross-section comparison between simulations and tests of clinching processes.

3. Computational and Experimental Studies of Tensile-shear Failure of Clinched Joints

It can be seen from Fig. 3, during the clinching process, the upper sheet undergoes a significant thinning near the punch corner radius. The strength of a clinched joint depends on the joint profile and particularly on the final thickness of the upper sheet near the punch corners, namely neck thickness, and the magnitude of the

produced undercut. The typical failure modes of clinched joints are, depend on the joint profile and loading conditions, the neck fracture mode and button separation mode as shown in Fig. 7.

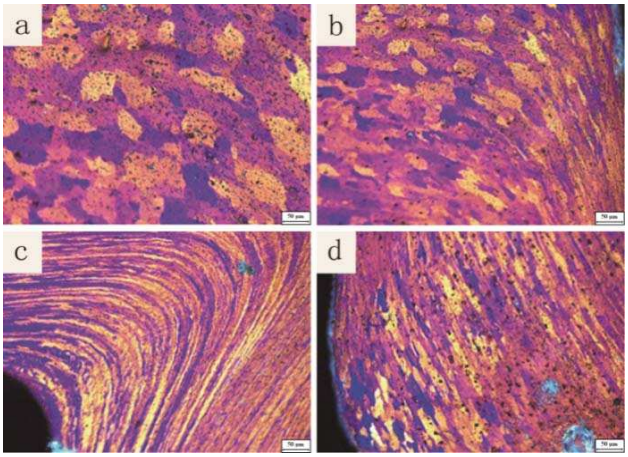

Fig. 6. Microstructure variations on the cross-section of clinched specimen in: (a) un-deformed zone; (b) mechanically affected zone; (c) sheet-sheet contacted zone and (d) sheet-die contacted zone.

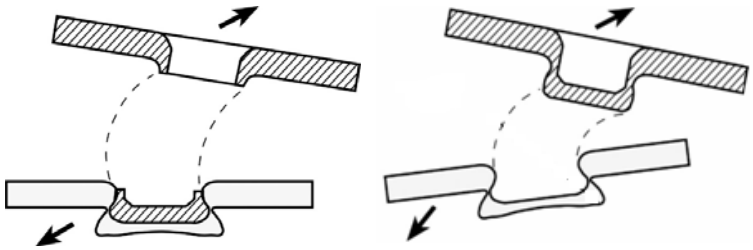

(a). Neck fracture mode (b). Button separation mode

Fig. 7. Typical failure modes of clinched joints

3.1 Numerical simulation of tensile-shear failure of clinched joints

A 3D model was generated using the commercial FE software ANSYS. The clinched joint was modelled using Solid187 solid elements. As the failures of a clinched joint usually occur around the clinch point inside the upper sheet, the FE mesh must accommodate both the small dimension of the clinch point and the larger dimension of the remainder of the whole joint. The original FE mesh is shown in Fig. 8. Input into the program was the description of 27550 elements by indicating the material properties for the elements. In the present study, a concentrated load of 2385 N (mean load value from tensile-shear test of 8 clinched specimens) was applied at the right end of the upper sheet as shown in Fig. 1.

The stress distributions around the clinch point in the clinched joint are given by the stress contour in Fig. 9. This stress contour shows that the upper sheet is subjected to high stress than the lower sheet and the maximum stress occurs at the neck of upper sheet. It is well known that in the tensile-shear tests the deformation of the joints is localized in the vicinity of the clinch point. In order to save CPU time, the numerical simulation of the tensile-shear failure of clinched joints can be axisymmetric, ignoring the exact geometry of the assembled sheets far from the clinch point. The tensile-shear failure process of the upper sheet of the clinched joint was also shown in Fig. 9.

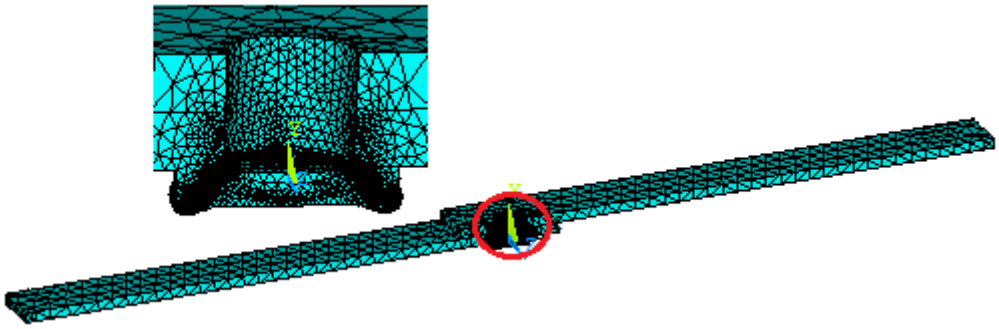

Fig. 8. 3D model of clinched joint

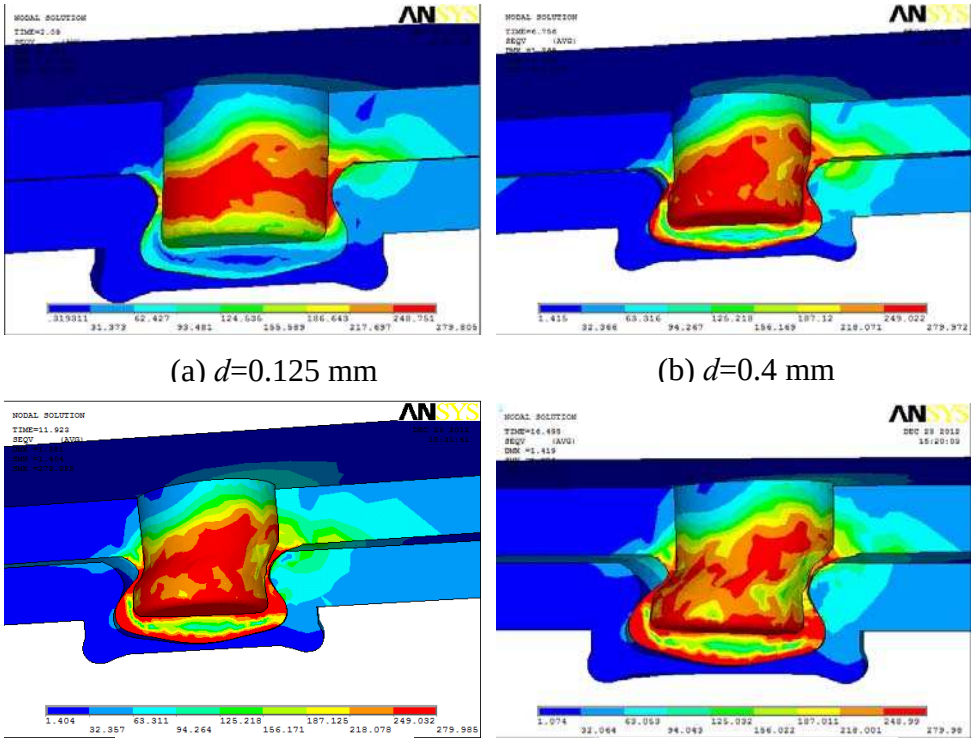

(a) d=0.125 mm (b) d=0.4 mm

(c) d=0.7 mm (d) d=0.98 mm

Fig. 9. Stress contour around the clinched point in tensile-shear failure process of the clinched joint (d represents the deformation in load

3.2 Tensile-shear test of clinched joints

A servo-hydraulic testing machine with hydraulic grips was used for conducting tensile-shear tests of clinched joints. The grip to grip specimen length was about 100 mm. The upper end of the joints was fixed, and a quasi-static downward displacement was applied to the lower end. For all clinched joints, spacers with the sheet thickness were used to centralise the load during testing. The tests were performed with a constant displacement rate of 1 mm/min. Continuous records of the applied force-displacement curves were obtained during each test. Table 1 shows the tensile-shear test results of clinched joints. Figures 10 and 11 show the tensile-shear process and failure model of the clinched joints separately.

Table 1. Tensile-shear test results of clinched joints

Specimens	Maximum load (N)	Energy absorption (J)
c-1	2356.00	0.823
c-2	2434.21	0.86
c-3	2334.25	0.825
c-4	2355.87	0.928
c-5	2408.51	0.873
c-6	2467.58	0.928
c-7	2340.66	1.013
c-8	2385.02	0.81

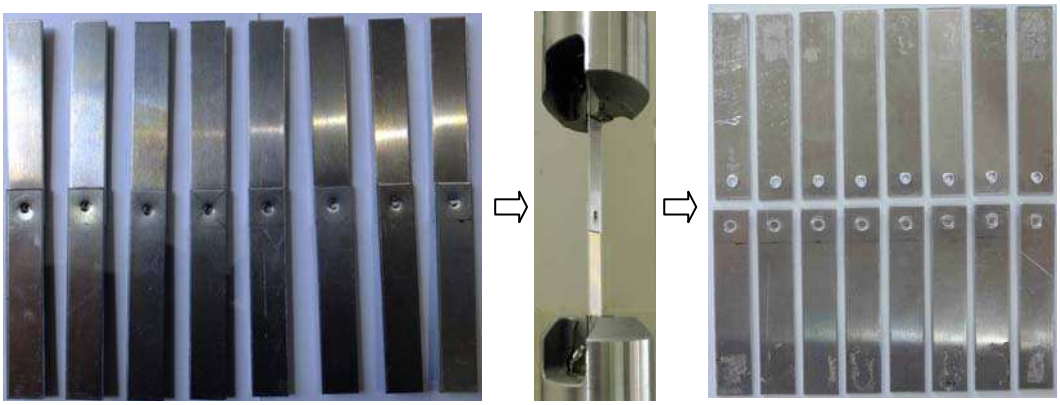

Fig. 10. Tensile-shear process of the clinched joints

Fig. 11. Failure mode of the clinched joints

As expected, it can be seen from figures 10 and 11 that in this case the failure mode is neck fracture mode which agree with the simulation results. Under the tensile-shear load, a main shear load is applied on the neck of upper sheet by geometrical interlocking and increasing gradually. The neck is fractured when the shear stress reaches the fracture stress of the upper sheet. The experimentally measured results were compared with the simulated results and found to be very well correlated.

4. Load-bearing Capacity and Energy Absorption of Clinched and Clinch-bonded Joints

Load-bearing capacity and energy absorption are two most important features in clinched joints structural analysis. It is also important for clinching to benefit from the advantages of other joining techniques, such as adhesively bonding. It is commonly understood that the addition of adhesive in clinched joints is beneficial but it is not clear if there are negative effects on mechanical properties of clinched joints [17]. In this section, deformation and failure of homogeneous joints under tensile-shear loading were studied for validating the load-bearing capacity and energy absorption of clinched joints and clinch-bonded hybrid joints.

The clinch-bonded hybrid joints were produced following exactly the same procedure as the respective clinched joints. The adhesive was applied on degreased surfaces and the two sheets were pressed together in order to squeeze sufficient adhesive out to avoid undue quilting of the finished clinch-bonded hybrid joints. The clinching processes were then produced. The thickness of the adhesive layer was controlled by the clinching process. Thereafter, the adhesive was cured at room temperature for at least 24 hours.

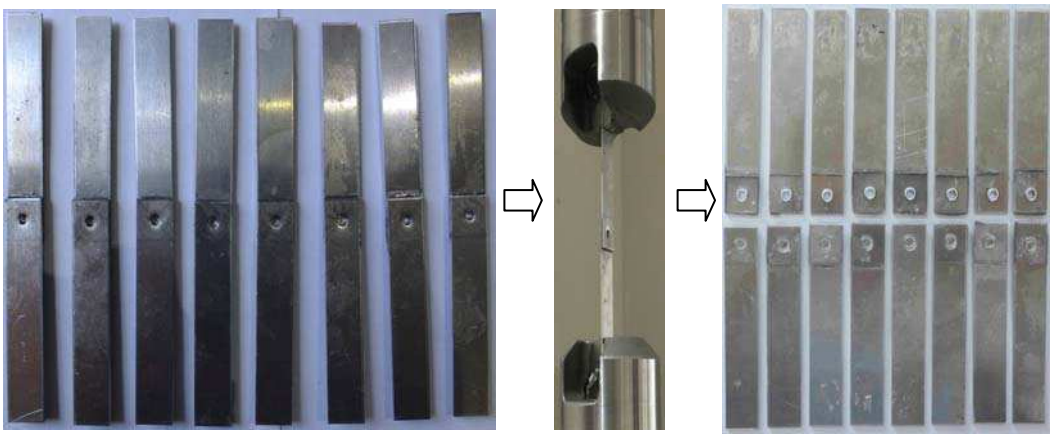

Fig. 12. Tensile-shear process of the clinch-bonded hybrid joints

The tensile-shear tests of clinch-bonded hybrid joints were performed with exactly the same procedure as the respective clinched joints. Fig. 12 shows the tensile-shear process of the clinch-bonded hybrid joints. It can be seen from Fig. 12 that the failure mode of the clinch-bonded hybrid joints is also neck fracture mode. Table 2 shows tensile-shear testing results of clinch-bonded hybrid joints.

Table 2. Tensile-shear testing results of clinch-bonded hybrid joints

Specimens	Maximum load (N)	Energy absorption (J)
h-1	2396.40	1.208
h-2	2422.33	1.169
h-3	2441.79	1.1
h-4	2446.69	1.14
h-5	2224.74	1.06
h-6	2522.04	1.223
h-7	2450.30	1.125
h-8	2550.94	1.285

Fig. 13 shows the force-displacement curves of the clinched joints and clinch-bonded hybrid joints. For each test, eight samples were mechanically tested. To examine the rationality of the test data, the normal hypothesis tests were performed using MATLAB 7.0. The results show that the tensile-shear strengths of all the clinched joints and clinch-bonded hybrid joints follow normal distributions. The mean values (μ) and standard deviations (σ) have the following numerical values: for clinched joints μ_{C}=2385.30 N, σ_{C}=47.85 N; for clinch-bonded joints μ_{CB}=2431.90 N, σ_{CB}=97.99 N. All test data fitting the region estimated by the degree of confidence of 95%. The tensile-shear strengths normal probability density distributions of the clinched joints and clinch-bonded hybrid joints are also shown in Fig. 13.

The energy absorption values of the clinched joints and clinch-bonded hybrid joints were obtained by measuring the areas between the force-displacement curves and abscissas. To examine the rationality of the energy absorption values of the clinched joints and clinch-bonded hybrid joints, the normal hypothesis tests were performed. The results show that the energy absorption values of all the clinched joints and clinch-bonded hybrid joints follow normal distributions. For clinched joints μ_{EAC} =0.8825 J, σ_{EAC} =0.0696; for clinch-bonded joints μ_{EACB} =1.1636 J, σ_{EACB}=0.0727. All test data fitting the region estimated by the degree of confidence of 95%. The energy absorption values normal probability density distributions of the clinched joints and clinch-bonded hybrid joints shown in Fig. 14.

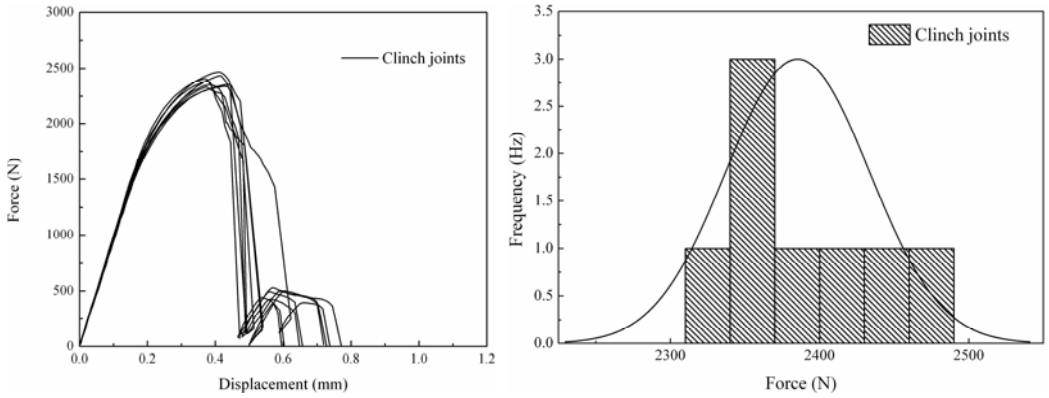

(a) Clinched joints

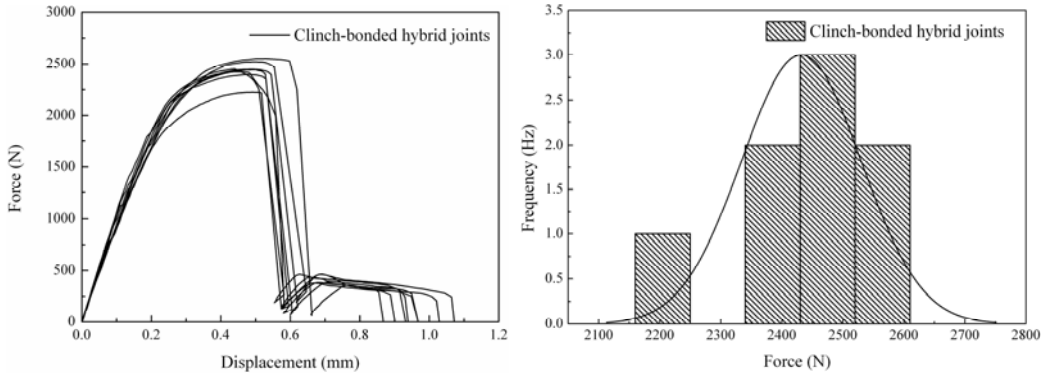

(b) Clinch-bonded hybrid joints

Fig. 13. Force-displacement curves and tensile-shear strengths normal probability density distributions of clinched joints and clinch-bonded hybrid joints

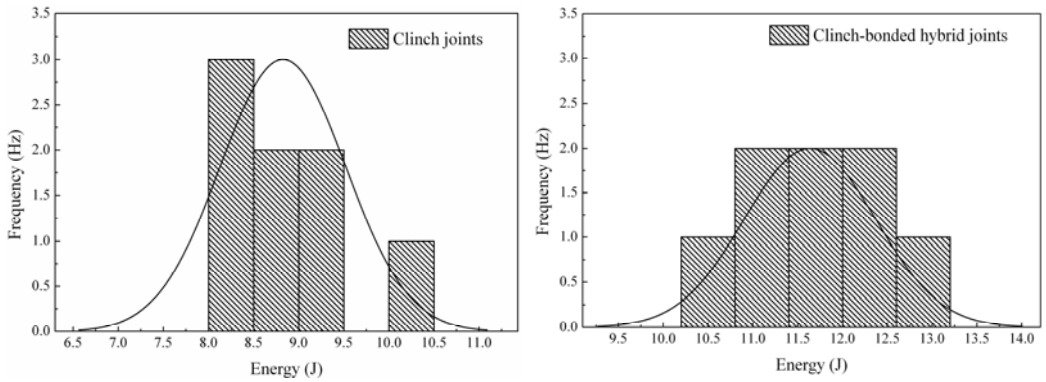

Fig.14. Energy absorption normal probability density distributions of clinched joints and clinch-bonded hybrid joints.

5. Discussion

Fig. 15 shows the intercept for load-bearing capacity and energy absorption of the clinched joints and clinch-bonded hybrid joints. It is clear that both the maximum load and energy absorption values of clinch-bonded hybrid joints are higher than that of clinched joints. This means that the addition of adhesive resulted in an increase in both the load-bearing and the energy absorption capacities of clinched joints. Table 3 shows statistical tensile-shear testing data of clinched joints and clinch-bonded hybrid joints.

Table 3. Statistical tensile-shear testing data of clinched joints and clinch-bonded hybrid joints

	Mean values	Standard deviations	Confidence interval (95%)
Maximum load of clinched joints	2385.3 (N)	47.85	2345.3-2425.3 (N)
Maximum load of hybrid joints	2431.9 (N)	97.993	2350-2513.8 (N)
Energy absorption of clinched joints	0.8825 (J)	0.0696	0.8244-0.9407 (J)
Energy absorption of hybrid joints	1.1636 (J)	0.0727	1.1028-1.2244 (J)

As mentioned above, the clinching processes were produced before adhesive curing. In the clinching process, adhesive layer can be like a lubricant and fully sandwiched between two sheets. After curing, the adhesive layer can give strong adhesive forces between two sheets due to the adhesion mechanism. In the tensile-shear test, a main shear load is applied on the neck of upper sheet by geometrical interlocking and increasing gradually which led to excessive elongation in the region of the joint neck. After the peak load the failure of adhesive layer occurs in a brittle manner. In this case, though the clinching still keeps the sheets connected but the joint can only bear low load, resulting in some more elongation, as shown in Fig. 13.

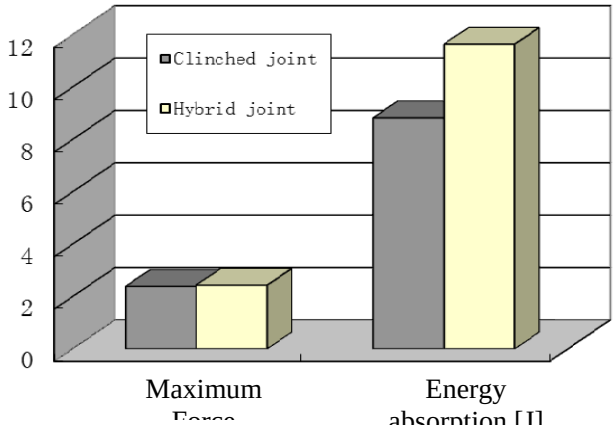

Fig. 15. Intercepts of strength and the energy absorption for clinched joints and clinch-bonded hybrid joints

6. Conclusions

The present paper aims to contribute to the basic studies on strength and energy absorption of clinched joints. The clinching process and tensile-shear failure of the clinched joints have been numerically and experimentally investigated. The results can be summarised as follows:

(1) The clinching process has been numerically simulated using a 2D LS-Dyna axisymmetric FE model. An implicit solution technique with Lagrange method and *r*-self-adaptivity was used. Experimental tests on specimens made of aluminium alloy 7075 have been carried out for validating the numerical simulations. Good agreements between the simulations and the tests have been found.

(2) The tensile-shear failure of the clinched joints has been numerically and experimentally investigated. In 3D FE numerical simulation, the stress contour shows that the upper sheet is subjected to high stress than the lower sheet and the maximum stress occurs at the neck of upper sheet. The tensile-shear failure process of the upper sheet has been presented. The experimentally measured results were compared with the simulated results and found to be very well correlated.

(3) Deformation and failure of homogeneous clinched joints under tensile-shear loading were studied for validating the load-bearing capacity and energy absorption of the clinched joints and clinch-bonded hybrid joints. The results show that the failure mode of the clinch-bonded hybrid joints is also neck fracture mode, the same as the clinched joints. The results also show that both maximum loads and energy absorption values of clinch-bonded hybrid joints are higher than that of clinched joints. This means that the addition of adhesive resulted in an increase in both the load-bearing and the energy absorption capacities of clinched joints.

(4) To examine the rationality of the test data, the normal hypothesis tests were performed using MATLAB 7.0. The results show that the tensile-shear strengths of all the clinched joints and clinch-bonded hybrid joints follow normal distributions. The results also show that the energy absorption values of all the clinched joints and clinch-bonded hybrid joints follow normal distributions.

Acknowledgement

This study is partially supported by National Natural Science Foundation of China (Grant No. 50965009) and the Special Program of the Ministry of Science and Technology, China (Grant No. 2012ZX04012-031).

References

[1] X. He, I. Pearson, K. Young, J Mater Process Tech. 199 (2008) 27-36.

[2] J. Mucha, Mater Des. 32 (2011) 4943-4954.

[3] J. Mucha, Mater Des. 52 (2013) 932-946

[4] X. He, F. Gu, A. Ball, Int J Adv Manufact Tech. 58 (2012) 643-649.

[5] X. He, Int. J. Adv. Manuf. Technol. 48 (2010) 607-612.

[6] X. He, Application of Finite Element Analysis in Sheet Material Joining, In: David Moratal (Ed). Finite Element Analysis - From Biomedical Applications to Industrial Developments, InTech., 2012, pp. 343-368.

[7] S. Gao, L. Budde, Int. J. Mach. Tools. Manuf. 34 (1994) 641-657.

[8] J. Zheng, X. He, J. Xu, K. Zeng, Y. Ding, Y. Hu, Adv. Mater. Res. 577 (2012) 9-12.

[9] T. Kuhne, 2008. Adhäs. Kleb. Dicht. 4 (2008) 24-27.

[10] F. Lambiase, A. Di Ilio, J. Mater. Eng. Perform. 22 (2013) 1629-1636.

[11] F. Lambiase, Int. J. Adv. Manuf. Tech. 66 (2012) 2123-2131.

[12] J.P. Varis, J. Mater. Process. Technol. 132 (2003) 242-249.

[13] J.P. Varis, J. Mater. Process. Technol. 172 (2006) 130-138.

[14] J.P. Varis, J. Mater. Process. Technol. 174 (2006) 277-285.

[15] K. Mori, Y. Abe, T. Kato, J. Mater. Process. Technol. 212 (2012) 1811-1988.

[16] X. He, Y. Ding, H. Yang, B. Xing, J VibroEng. In press.

[17] X. He, Int. J. Adhes. Adhes. 31 (2011) 248-264.